Supporting Information

Mapping the surface electronic landscape of solution-processed CuIn(S,Se)2 thin-films as a function of the Cu/In ratio

Ye Ma,[1] Alice Sheppard,[1,2] Jacques D. Kenyon,[3] Jude Laverock,[1] Nada Benhaddou,[3] Valentina Corsetti,[1] Jake W. Bowers,[3] David J. Fermin[1]*

[1] School of Chemistry, University of Bristol, Cantocks Close, BS8 1TS Bristol, United Kingdom.
[2] H. H. Wills Physics Laboratory, University of Bristol, Tyndall Avenue, BS8 1TL Bristol, United Kingdom.
[3] Centre for Renewable Energy Systems Technology (CREST), Wolfson School of Mechanical Electrical and Manufacturing Engineering, Loughborough University, Loughborough, LE11 3TU, United Kingdom

Corresponding author

David J. Fermin: david.fermin@bristol.ac.uk

Experimental Methods

CIS Precursor Solution Preparation. The preparation of the precursor solution was performed in an argon-filled glovebox (Ossila Ltd.) at room temperature. Thiourea (TU, Sigma Aldrich, 98%), copper(I) chloride (CuCl, Merk, > 99.99%), and indium(III) chloride ($InCl_3$, Thermo Fisher, 99.99%) were sequentially added into a binary solvent mixture of DMF and IPA in a 75:25 volume ratio. Each salt was sonicated until fully dissolved. The total concentration was kept at 2.8 M and the molar ratio of TU/(Cu+In) was fixed at 5. The Cu/In molar ratios were chosen at 0.85, 0.95, 1.00 and 1.10 to study the effect of Cu/In ratios.

CISSe Thin Film Fabrication. Commercial Molybdenum-coated soda-lime glass substrates (AimCore) were cleaned by sequential sonication in deionized water (DI), acetone and DI for 10 minutes each, and then dried with pressurized argon. The cleaned substrates were treated under UV-Ozone (Jelight UVO-Cleaner Model) for 20 minutes. The precursor solution was spin-coated at 2000 rpm for 60 s onto Mo/SLG substrate, followed by annealing at 350 °C for 120 s and cool down to room temperature. This process was repeated 13 times to achieve a precursor film thickness of 480–580 nm. The precursor film was subsequently put into a graphite box with 300 mg Se and 100 mg SeS_2 powder and annealed in a rapid thermal annealing furnace (MTI OTF-1200X). The furnace was heated at a ramp rate of 1.8 °C/s to 560 °C and held at this temperature for 30 minutes under a constant Argon flow of 28 sccm (1 atm). The CISSe absorbers were removed from the furnace once it cooled to 50 °C.

Device Fabrication. CISSe solar devices were completed by the deposition of a 50 nm of CdS using chemical bath deposition, a 50 nm of i-ZnO and 500 nm of Al-doped ZnO (AZO) via radio frequency (RF) sputtering. 500 nm of Ag top electrode was deposited by thermal

evaporation. The 0.25 cm^2 device area was defined through mechanical scribing. According to bulk Cu/In ratio detected by XRF, the absorbers and solar cell devices are denoted as Cu/In-0.80, Cu/In-0.95, Cu/In-1.00, Cu/In-1.10, respectively.

Film Characterization. X-ray fluorescence (XRF) was measured using Bruker, Mistral M1. The instrument was initially calibrated using a fundamental parameter (FP) method based on the elemental ratios within the CIS layer. The reported results represent the average of measurements taken over a 3*3 matrix, with each point measured for 200 seconds. The current-voltage (I-V) characteristics were measured by a solar meter (Keithley 4200-SCS) and a solar simulator (Wavelabs Sinus-70 light) under an AM 1.5G spectrum (100mW/cm^2, 25 °C). The photovoltaic parameters were extracted from Lambert W-based curve fitting algorithm of J-V characteristics using Matlab. The J_{sc} values extracted from EQE is, on average, 2.8 mA cm^{-2} higher (<10%) than the J-V measurements, which is attributed to the mask and measurement probe shading. The external quantum efficiency (EQE) spectrum was obtained from a Betham PVE300 system with a dual halogen and single xenon as light sources at 0 V bias with 5 nm spectral resolution, and a transformer (x500 474 type pre-amp). It should be mentioned that the $V_{OC,def}$ was calculated considering the band gap values extracted from the EQE spectra in **Figure 1e,** which is slightly larger than the top efficiency cells. Raman spectra (Renishaw inVia) were obtained using a 488 nm excitation wavelength laser. X-ray diffraction (XRD) patterns were required by a Bruker D8 Advance instrument equipped with a Cu Kα (λ = 1.54184Å) X-ray source. Top-down and cross-sectional absorber morphology was imaged by scanning electron microscopy (SEM) (Jeol IT300 SEM). X-ray photoelectron spectroscopy (XPS), energy-filtered photoemission electron microscopy (EF-PEEM) and ultraviolet photoelectron spectroscopy (UPS) were conducted using NanoESCA II (ScientaOmicron/FOCUS) under ultra-high vacuum (UHV, base pressure of 4×10^{-11} mbar). CISSe absorbers were pre-treated using Ar^+ plasma at 0.5 kV for 6 minutes for sample preparation in order to remove surface contaminants. The XPS instrument uses an Argus (ScientaOmicron) XPS analyzer and a monochromatic Al Kα (1486.7 eV) source, and pass energies of 100 eV and 50 eV were used for survey and core level analysis, respectively. The binding energy and intensity scales are well calibrated via clean polycrystalline metal films and low-density polyethylene,[1, 2] respectively. The Cu/In ratio was quantified by analyzing Cu 2p and In 3d spectra over a wide energy range above the main photoelectron peaks (> 130 eV for Cu 2p and > 80 eV for In 3d), allowing the background to be accurately evaluated using electron energy loss theory.[3] The resulting background-subtracted spectrum then contains all intrinsic photoelectron signals, including those arising from intrinsic plasmon excitations, shake-up and shake-off satellites. These spectra were then used to quantify the Cu/In ratio, where we employ Scofield photoelectron cross-sections,[4] corrected by the photoelectron angular distribution of our instrument geometry,[5] and including the effects of the different escape depths due to the different peak energies.[6] This procedure provides accurate experimental surface ratios without the need for external calibration samples.[7, 8] EF-PEEM was performed under He I light source (21.22 eV photon energy) with a spatial resolution of approximately 100 nm. The analyzer was operated with an energy resolution of 100 meV and pass energy of 50 eV. As described by He et al., the extracted work function (WF) is determined from $E–E_F$ at the photoemission energy threshold.[9] From a Gaussian fit,

the center of the WF distribution and the standard deviation can be extracted. Secondary ion mass spectrometry (SIMS) was performed using a Hidden Analytical gas-ion gun equipped with a quadrupole mass analyzer. A 4 keV O^+ primary beam was measured over a field of 500 μm^2 with the duty cycle of 10%.

Table S1. Summary of average device performance of CISSe solar cells with the absorbers fabricated as a function of the Cu/In ratio.

Cu/In ratio	PCE (%)	V_{oc} (mV)	J_{sc} (mA/cm^2)	FF (%)
0.80	7.0 ± 0.7	449 ± 22	25.7 ± 0.9	60.7 ± 2.9
0.95	8.8 ± 0.3	529 ± 7	25.2 ± 1.5	65.2 ± 2.5
1.00	8.0 ± 0.8	507 ± 8	25.1 ± 0.9	62.6 ± 4.4
1.10	5.5 ± 0.5	440 ± 14	20.4 ± 0.7	61.2 ± 4.4

Table S2. Cu/In ratios from prepared precursor solution and film measured from XRF.

Cu/In ratio – precursor solution	CISSe thickness (µm)	Cu (at%)	In (at%)	Cu/In ratio – XRF	Average Cu/In ratio - XRF
0.85	0.55	23.42	27.84	0.84	**0.80**
	0.54	22.52	29.45	0.76	
	0.55	22.92	28.75	0.80	
0.95	0.52	22.63	23.88	0.95	**0.94**
	0.52	22.33	25.87	0.86	
	0.52	23.39	23.43	0.99	
1.00	0.56	20.53	19.98	1.03	**1.00**
	0.55	19.36	20.15	0.97	
	0.55	20.78	20.51	1.01	
1.10	0.54	23.98	21.63	1.11	**1.10**
	0.53	24.74	22.24	1.11	
	0.55	23.57	21.74	1.08	

Table S3. Summary of best device performance of CISSe solar cells with the absorbers fabricated as a function of the Cu/In ratio.

Cu/In ratio	PCE (%)	V_{oc} (mV)	J_{sc} (mA cm^{-2})	FF (%)	$V_{oc,def}$ (mV)	J_{sc} from EQE (mA cm^{-2})	n	R_s (Ω cm^2)	R_{sh} (Ω cm^2)	J_0 (mA/cm^2)
0.80	7.9	478	26.0	63.6	486	27.3	1.51	1.68	469	1.2×10^{-4}
0.95	9.1	533	26.4	64.7	431	29.0	1.66	0.99	285	9.3×10^{-5}
1.00	8.9	522	26.1	65.4	451	28.7	1.39	1.44	330	1.8×10^{-5}
1.10	6.2	469	20.5	65.0	504	24.2	1.43	1.31	331	5.5×10^{-5}

Table S4. Surface Cu/In ratios of CISSe absorbers obtained from XPS, error of surface Cu/In ratio, WF center and standard deviation (Std. Dev.) from EF-PEEM, estimated from fitting with a Gaussian curve.

Bulk Cu/In ratio	Surface Cu/In ratio	Error of Surface Cu/In ratio	WF center (eV)	WF Std. Dev. (meV)
0.80	0.5935	0.0061	4.85	54
0.95	0.6108	0.0062	4.90	102
1.00	0.7439	0.0064	4.75	65
1.10	0.8047	0.0068	4.55	76

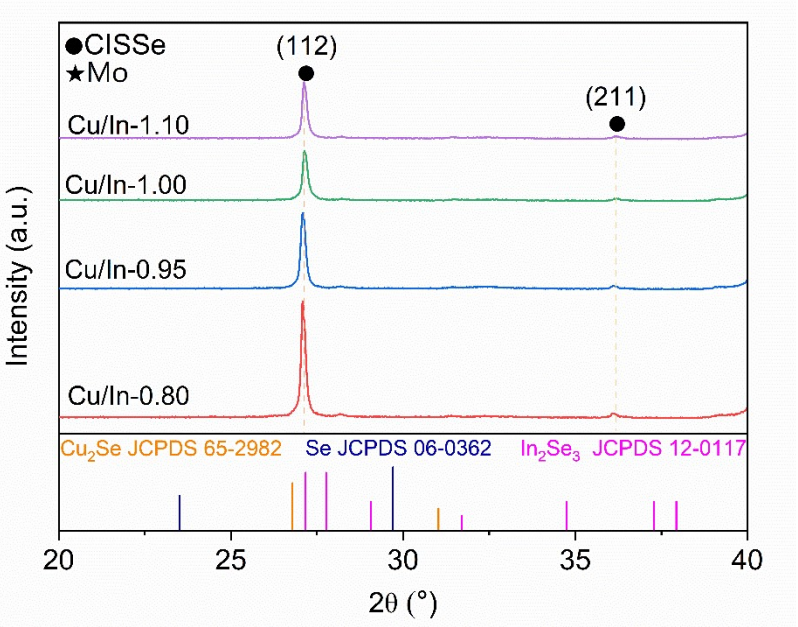

Figure S1. XRD patterns within 20-40° of Cu/In-0.80 (red), Cu/In-0.95 (blue), Cu/In-1.00 (green), Cu/In-1.10 films (purple), overlaid with reference patterns for Cu_2Se (orange), In_2Se_3 (pink) and elemental Se (royal blue) XRD card. We do not observe additional diffractions attributed to Cu_2Se and In_2Se_3 secondary phases in this range.

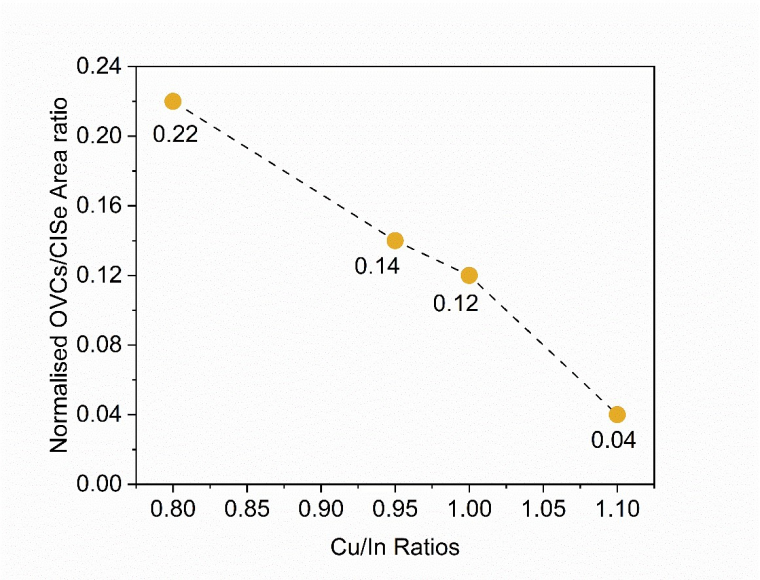

Figure S2. Normalized peak area of OVCs mode to CISe A^1 mode of each Cu/In ratio.

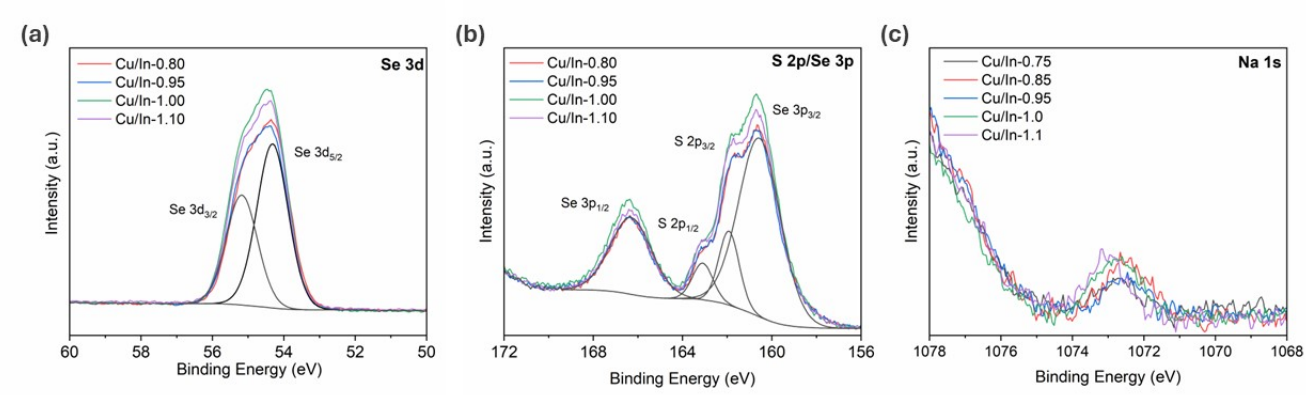

Figure S3. XPS spectra of (a) Se 3d, (b) S 2p/Se 3p, and (c) Na 1s of the CISSe absorbers of Cu/In-0.80 (red), Cu/In-0.95 (blue), Cu/In-1.00 (green), Cu/In-1.10 ratios (purple). Se 3d and S 2p/Se 3p were de-convoluted into $d_{3/2}$ and $d_{5/2}$ and $p_{1/2}$ and $p_{3/2}$, respectively.

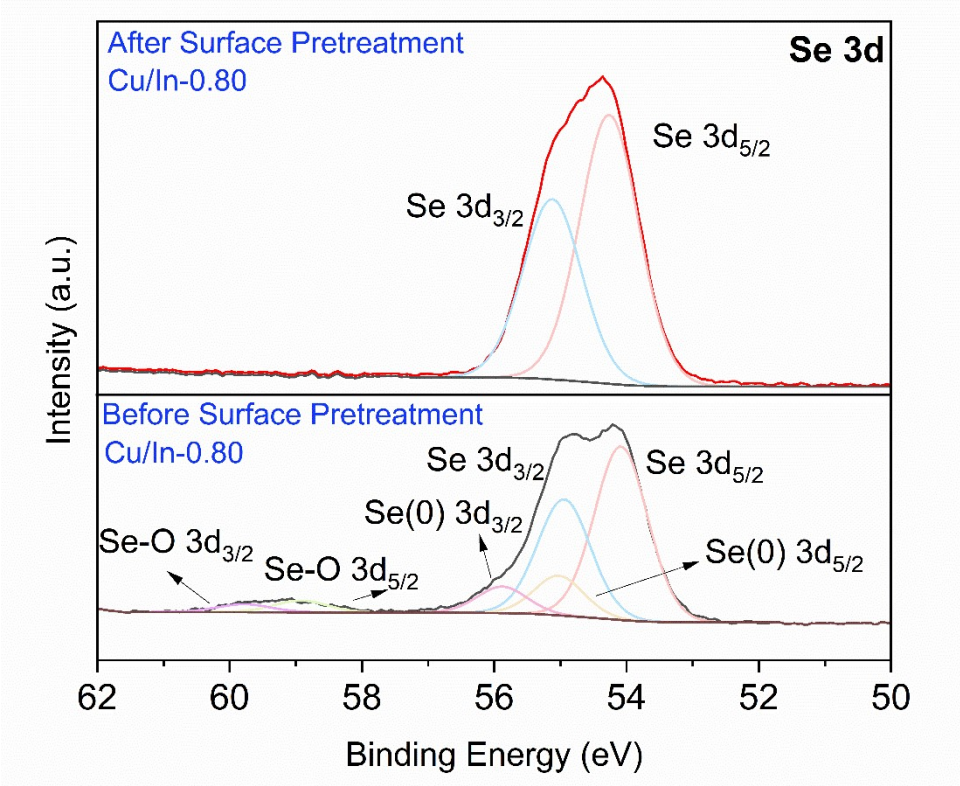

Figure S4. XPS spectra of Se 3d for Cu/In-0.80 absorber before (bottom) and after (top) surface pretreatment.

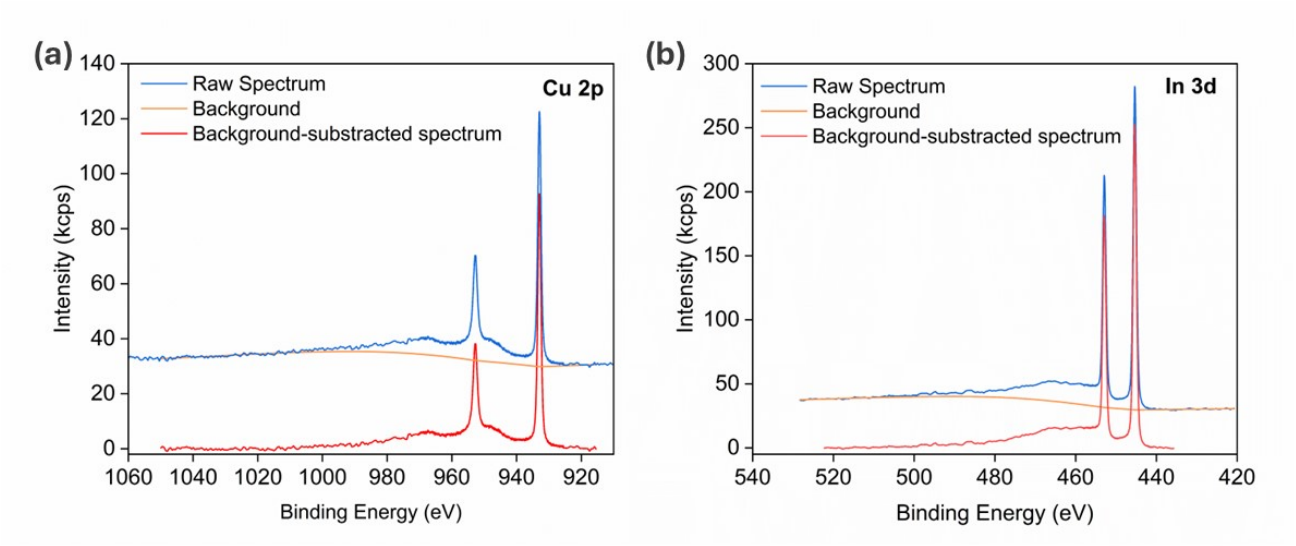

Figure S5. Extended (raw) spectrum (blue), background based on energy loss theory (orange), and background-subtracted spectrum used for quantification (red) of (a) Cu 2p and (b) In 3d of absorber Cu/In-1.00.

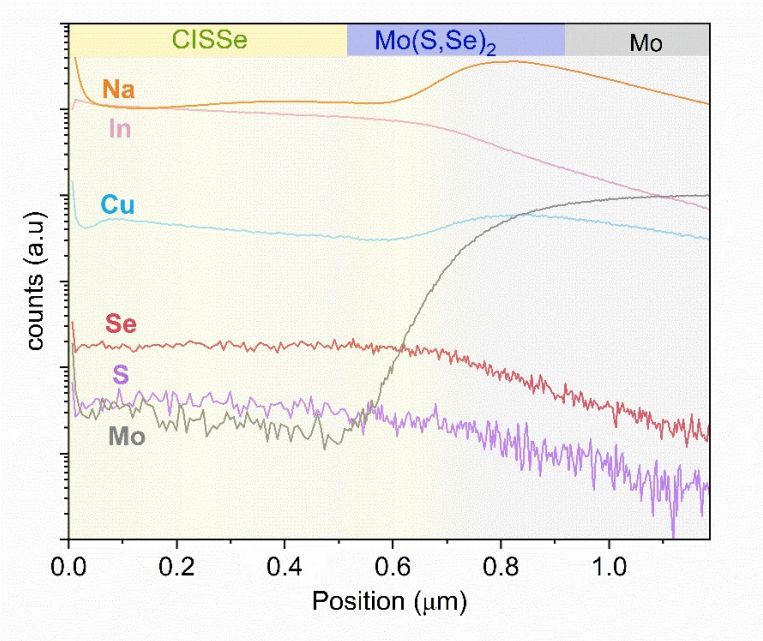

Figure S6. Secondary ion mass spectrometry (SIMS) profile of Cu/In-0.95 absorber.

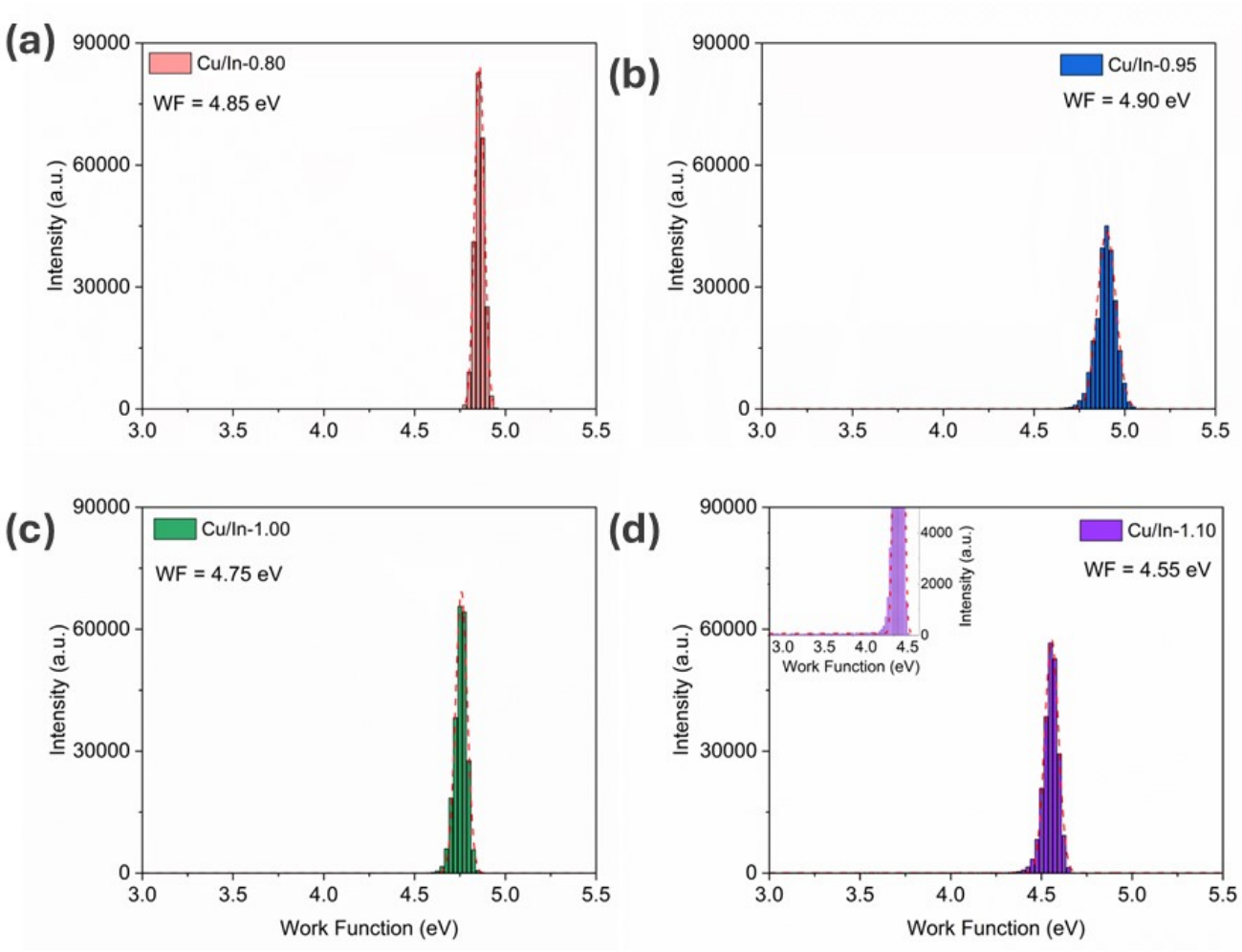

Figure S7. The WF histograms of the CISSe absorber of (a) Cu/In-0.80 (red), (b) Cu/In-0.95 (blue), (c) Cu/In-1.00 (green), (d) Cu/In-1.10 (purple).

References

1. A. G. Shard and B. P. Reed, Al Kα XPS reference spectra of polyethylene for all instrument geometries. *Journal of Vacuum Science & Technology A*, 2020, **38**
2. B. P. Reed, D. J. H. Cant, S. J. Spencer, A. J. Carmona-Carmona, A. Bushell, A. Herrera-Gómez, A. Kurokawa, A. Thissen, A. G. Thomas, A. J. Britton, A. Bernasik, A. Fuchs, A. P. Baddorf, B. Bock, B. Theilacker, B. Cheng, D. G. Castner, D. J. Morgan, D. Valley, E. A. Willneff, E. F. Smith, E. Nolot, F. Xie, G. Zorn, G. C. Smith, H. Yasufuku, J. L. Fenton, J. Chen, J. D. P. Counsell, J. Radnik, K. J. Gaskell, K. Artyushkova, L. Yang, L. Zhang, M. Eguchi, M. Walker, M. Hajdyła, M. M. Marzec, M. R. Linford, N. Kubota, O. Cortazar-Martínez, P. Dietrich, R. Satoh, S. L. M. Schroeder, T. G. Avval, T. Nagatomi, V. Fernandez, W. Lake, Y. Azuma, Y. Yoshikawa and A. G. Shard, Versailles Project on Advanced Materials and Standards interlaboratory study on intensity calibration for x-ray photoelectron spectroscopy instruments using low-density polyethylene. *Journal of Vacuum Science & Technology A*, 2020, **38**
3. S. Tougaard, Practical algorithm for background subtraction. *Surface Science*, 1989, **216**, 343-360

4. J. H. Scofield, Hartree-Slater subshell photoionization cross-sections at 1254 and 1487 eV. *Journal of Electron Spectroscopy and Related Phenomena*, 1976, **8**, 129-137
5. M. B. Trzhaskovskaya, V. I. Nefedov and V. G. Yarzhemsky, PHOTOELECTRON ANGULAR DISTRIBUTION PARAMETERS FOR ELEMENTS Z=1 TO Z=54 IN THE PHOTOELECTRON ENERGY RANGE 100–5000 eV. *Atomic Data and Nuclear Data Tables*, 2001, **77**, 97-159
6. P. J. Cumpson, Estimation of inelastic mean free paths for polymers and other organic materials: use of quantitative structure–property relationships. *Surface and Interface Analysis*, 2001, **31**, 23-34
7. A. G. Shard, Practical guides for x-ray photoelectron spectroscopy: Quantitative XPS. *Journal of Vacuum Science & Technology A*, 2020, **38**
8. S. Tougaard, Practical guide to the use of backgrounds in quantitative XPS. *Journal of Vacuum Science & Technology A*, 2020, **39**
9. Y. He, I. M. Vishik, M. Yi, S. Yang, Z. Liu, J. J. Lee, S. Chen, S. N. Rebec, D. Leuenberger, A. Zong, C. M. Jefferson, R. G. Moore, P. S. Kirchmann, A. J. Merriam and Z.-X. Shen, Invited Article: High resolution angle resolved photoemission with tabletop 11 eV laser. *Review of Scientific Instruments*, 2016, **87**